MASTER COPY KEEP THIS COPY FOR REPRODUCTION PURPOSES

# REPORT DOCUMENTATION PAGE

Form Approved
OMB No. 0704-0188



| 1. AGENCY USE ONLY (Leave blank) | 2. REPORT DATE | 3. REPORT TYPE AND DATES COVERED |
|---|---|---|
| | 12/31/94 | Final 6/1/91 - 12/31/94 |

**4. TITLE AND SUBTITLE**
Semiconductor deposition and etching interactions of laser-generated translationally hot atoms and radicals

**5. FUNDING NUMBERS**
DAAL03-91-G-0191

**6. AUTHOR(S)**
Stephen R. Leone

**7. PERFORMING ORGANIZATION NAME(S) AND ADDRESS(ES)**
Regents of the University of Colorado
Boulder, Colorado 80309-0019
(Joint Institute for Laboratory Astrophysics)

**8. PERFORMING ORGANIZATION REPORT NUMBER**



**9. SPONSORING / MONITORING AGENCY NAME(S) AND ADDRESS(ES)**
U.S. Army Research Office
P. O. Box 12211
Research Triangle Park, NC 27709-2211

**10. SPONSORING / MONITORING AGENCY REPORT NUMBER**
ARO 28561.7-PH

**11. SUPPLEMENTARY NOTES**
The views, opinions and/or findings contained in this report are those of the author(s) and should not be construed as an official Department of the Army position, policy, or decision, unless so designated by other documentation.

**12a. DISTRIBUTION / AVAILABILITY STATEMENT**
Approved for public release; distribution unlimited.

**12b. DISTRIBUTION CODE**



**13. ABSTRACT** *(Maximum 200 words)*

Laser vaporization of cryogenic films is employed to produce translationally fast atoms and radicals, and these kinetic-energy-enhanced species are used for studies of semiconductor etching; the results are important for the basic physics of electronics materials processing. Recent accomplishments include (1) production of a novel source of kinetic-energy-enhanced beams of $Cl_2$, Cl, and F atoms by laser vaporization, (2) observation of substantial enhancement of the etching rate and sustained etching of room temperature Si(100) by chlorine molecules with energies ≥3 eV, (3) scattering studies of translationally fast $Cl_2$ and Cl with Si(100), (4) velocity selection of the translationally fast beams for energy-resolved studies of dry etching processes, and (5) measurements of $SiCl_x$ product distributions as a function of substrate temperature.



| 14. SUBJECT TERMS | 15. NUMBER OF PAGES |
|---|---|
| semiconductor, etching, neutrals, beams, scattering | 32 |
| | 16. PRICE CODE |

| 17. SECURITY CLASSIFICATION OF REPORT | 18. SECURITY CLASSIFICATION OF THIS PAGE | 19. SECURITY CLASSIFICATION OF ABSTRACT | 20. LIMITATION OF ABSTRACT |
|---|---|---|---|
| UNCLASSIFIED | UNCLASSIFIED | UNCLASSIFIED | UL |

## Table of Contents

## Final Report

## Recent Publications Sponsored By ARO


L. M. Cousins and S. R. Leone, "Production of 0.1-3 eV reactive molecules by laser vaporization of condensed molecular films: A potential source for beam-surface interactions," J. Materials Res. **3**, 1158 (1988).

L. M. Cousins and S. R. Leone, "Time-of-flight measurements of hyper-thermal $Cl_2$ molecules produced by UV laser vaporization of cryogenic chlorine films," Chem. Phys. Lett. **155**, 162 (1989).

L. M. Cousins, R. J. Levis, and S. R. Leone, "Observation of translationally hot, rotationally cold NO molecules produced by 193-nm laser vaporization of multilayer films," J. Phys. Chem. **93**, 5325 (1989).

L. M. Cousins, R. J. Levis, and S. R. Leone, "Translational and internal state distributions of NO produced in the 193 nm explosive vaporization of cryogenic NO films: Rotationally cold, translationally fast NO molecules," J. Chem. Phys. **91**, 5731 (1989).

R. J. Levis, C. J. Waltman, L. M. Cousins, R. G. Copeland and S. R. Leone, "A hyperthermal (0.1-4 eV) F atom beam source suitable for surface etching investigations," J. Vac. Sci. Technol. A **8**, 3118 (1990).

F. X. Campos, G. C. Weaver, C. J. Waltman, and S. R. Leone, "Activation of the $Si(100)/Cl_2$ etching reaction at high $Cl_2$ translational energies," Mat. Res. Symp. Proc. **236**, 177 (1992).

F. X. Campos, G. C. Weaver, C. J. Waltman, and S. R. Leone, "Enhanced etching of Si(100) by neutral chlorine beams with kinetic energies up to 6 eV," J. Vac. Sci. Technol. B **10**, 2217 (1992).

F. X. Campos, C. J. Waltman, and S. R. Leone, "Laser vaporization time-of-flight studies of cryogenic $Cl_2$/Xe films," Chem. Phys. Lett. **201**, 399 (1993).

G. C. Weaver, F. X. Campos, and S. R. Leone, "Hyperthermal Cl atom beam produced by laser vaporization of cryogenic ICl films," Mat. Res. Symp. Proc. **285**, 249 (1993).

G. C. Weaver and S. R. Leone, "Scattering of $Cl_2$ beams from Si(100) for kinetic energies up to 2.6 eV: Implications for sticking coefficients and reaction product formation," Surface Sci. (in press).

S. R. Leone, F. X. Campos, and G. C. Weaver, "Silicon etching by kinetic-energy-enhanced chlorine," Proceedings of the 1994 Symposium on Dry Process, p. 85, Tokyo, Japan (1994).

S. R. Leone, "Kinetic-energy-enhanced neutral etching," Jpn. J. Appl. Phys. (submitted).

G. C. Weaver and S. R. Leone, "Atomic fragments produced by laser vaporization," in preparation, Chem. Phys. Lett.

## Introduction

This is a report to the Physics Division of the Army Research Office of results concerning the mechanisms of dry etching by translationally "hot" atoms and molecules. With support from the current ARO grant, a new beam source of translationally fast neutral reactive atoms, radicals, and molecules (typically 1-5 eV) was developed and characterized.[1-5] This beam source was used in first experiments to investigate the mechanisms of dry etching of silicon by kinetic-energy-enhanced chlorine.[6,7] Sustained etching of room temperature silicon by the fast beams is observed, as well as differences in the predominant etch products that are usually reported. The results are central to the functioning of electron cyclotron resonance (ECR) plasma etch reactors, in which enhanced kinetic energy neutral species are known to be important.[8-11]

The beam source is based on the laser vaporization technique, utilizing cryogenic films deposited continuously. The mechanisms of laser vaporization have been studied by many groups in the past several years.[12-30] Laser vaporization can be used to produce a variety of reactive neutral atoms, radicals, metal vapors, and other compounds with high kinetic energies, and even to launch large macromolecules into the gas phase for analysis and detection. There are also many direct applications of laser vaporization and ion ablation processes which are used to remove materials for electronics processing.[18,19,21,31-39] In this work the laser vaporization process is employed to produce a beam source of energetic, reactive neutral species (typically 1-5 eV) which is used to study collisions with semiconductor surfaces for fundamental investigations of the mechanisms of etching. In a similar context, a laser-sustained plasma source has also been reported for anisotropic etching of photoresists by translationally fast O atoms.[40]

## Motivation for Studies of Dry Etching by Fast Neutral Particles

There is widespread interest in the elucidation of the mechanisms of dry etching processes for the manufacture of submicron features in semiconductor devices.[34,35,37-39,41-49] State-of-the-art techniques couple the chemical specificity of reactive species, which remove materials selectively, with the anisotropic characteristics of ion bombardment to produce sharp sidewall profiles. For example, consider the etching of silicon by $XeF_2$ in the presence of $Ar^+$ bombardment.[50] In

this case the chemical nature of the fluorine species gives elemental discrimination, resulting in chemical etching of silicon. The Ar ion bombardment has little selectivity for particular elements, but it provides for directed-area removal of etching products or the supply of energy to overcome activation barriers in the reactions involved in material removal. The use of high energy ion bombardment, however, can produce damages, which are undesirable.[39,51,52] These include displacements of atoms in the semiconductor lattice, formation of electron-hole pairs, surface contamination by redeposition, and incorporation of impurities from the ion source. These damages are particularly troublesome in the limit of ultrasmall devices in which electrons are confined to dots or wires that are smaller than the wavelengths of the electron and for ultrathin gate oxide materials in MOS semiconductors.[52]

The use of ion bombardment to enhance etching rates suggests that in many cases there are barriers to desorption or in the reactions that form the products. Etching by low energy species, such as F or Cl alone, which are some of the primary etchant radicals in plasma etching, produces little selectivity in direction;[53,54] it is now known, however, that translationally fast neutral species are also formed in plasma reactors, either by ion exchange reactions or dissociation reactions, and these can play an important role in plasma etching.[8-11,42,43] This is particularly true for the low pressure ECR types of plasmas, which are currently exploited in many applications. What is not known is whether the translationally fast neutral species enhance or diminish the anisotropy of the etching, and what role they play to increase the rates of etching. For example, in recent studies of O atom etching of photoresists,[40] anisotropic etching is attributed to the increased kinetic energy. In other reports, enhanced kinetic energy is considered to be deleterious to the anisotropy of the etching.[10] Thus, it is important to understand the role of moderate kinetic energy (1-10 eV) reactive neutral particles emanating from these plasma etch reactors and how they influence the etching rates and anisotropies as a function of substrate temperature. If possible, an important benefit of lower temperature processing will be smaller features in semiconductors of the future.

There are also reports of etching with both vibrationally excited $SF_6$ and $Cl_2$ molecules[48,55] and hot radicals and molecules (F, Cl, $CH_3$) formed by thermal decomposition of molecules in a "hot jet".[56] While there is some controversy about

whether these processes are due to enhanced vibrational or kinetic energy, or even due to radicals formed by thermal cracking, these publications are of particular interest since they do suggest that species with elevated vibrational or kinetic energies can etch materials directly by themselves. In some cases this occurs with reasonable anisotropies. Theoretical calculations also find that collisions of beams of 5-10 eV Si atoms with a Si surface promote nonthermal growth of the semiconductor by direct insertion into the solid via bond breaking and forming mechanisms.[57] These results provide encouraging reasons to study etching and deposition with translationally fast atoms and radicals. In studies here, we produce these fast species by laser vaporization techniques.

## Research Progress (1 June 1991 - 31 December 1994)

In the past three years, new experiments have been performed to characterize the laser vaporization process and to carry out etching studies of translationally fast species with semiconductor surfaces. In the sections below, we discuss the apparatus and the most recent results performed to analyze the vaporization process and to characterize the etching of silicon by 1-6 eV chlorine molecules.

### Apparatus for Semiconductor Etching

An apparatus was designed to produce translationally fast beams of reactive atoms and molecules by pulsed laser vaporization of material from cryogenically condensed films and to use these beams for semiconductor etching studies (Fig. 1 below).[7] The source material for the beam is deposited continuously on a transparent substrate at 20 K, so that the pulsed beam is repetitive. The pulsed beam flux may be chopped with a single slotted chopper to select the kinetic energy. The relative flux of the beam is measured with a fast ionization gauge for normalization purposes. The translationally hot beams pass into an ultrahigh vacuum (UHV) chamber, where the scattering and etching studies take place. The kinetic energy of the incident beam is analyzed by time-of-flight measurements with the line-of-sight quadrupole mass spectrometer, and the scattered species are detected at right angles with a second quadrupole mass spectrometer when the substrate is inserted. A semiconductor substrate, usually Si(100), is mounted on the sample manipulator and can be heated by electron bombardment. The substrate's cleanliness and

oxidation state are determined by X-ray photoelectron spectroscopy or Auger, and cleaning is accomplished with mild Ar ion sputtering and heating.

The beam source works as follows. A transparent substrate is mounted on the helium refrigerator. Molecules such as $Cl_2$, $XeF_2$, or ICl from a doser are condensed continuously on the substrate by cryogenic deposition. High energy pulses from a frequency doubled, tripled or quadrupled Nd:YAG laser (532, 355 or 266 nm, respectively) are directed through the window either from the front or the back of the growing film to vaporize the coating and eject translationally "hot" molecules

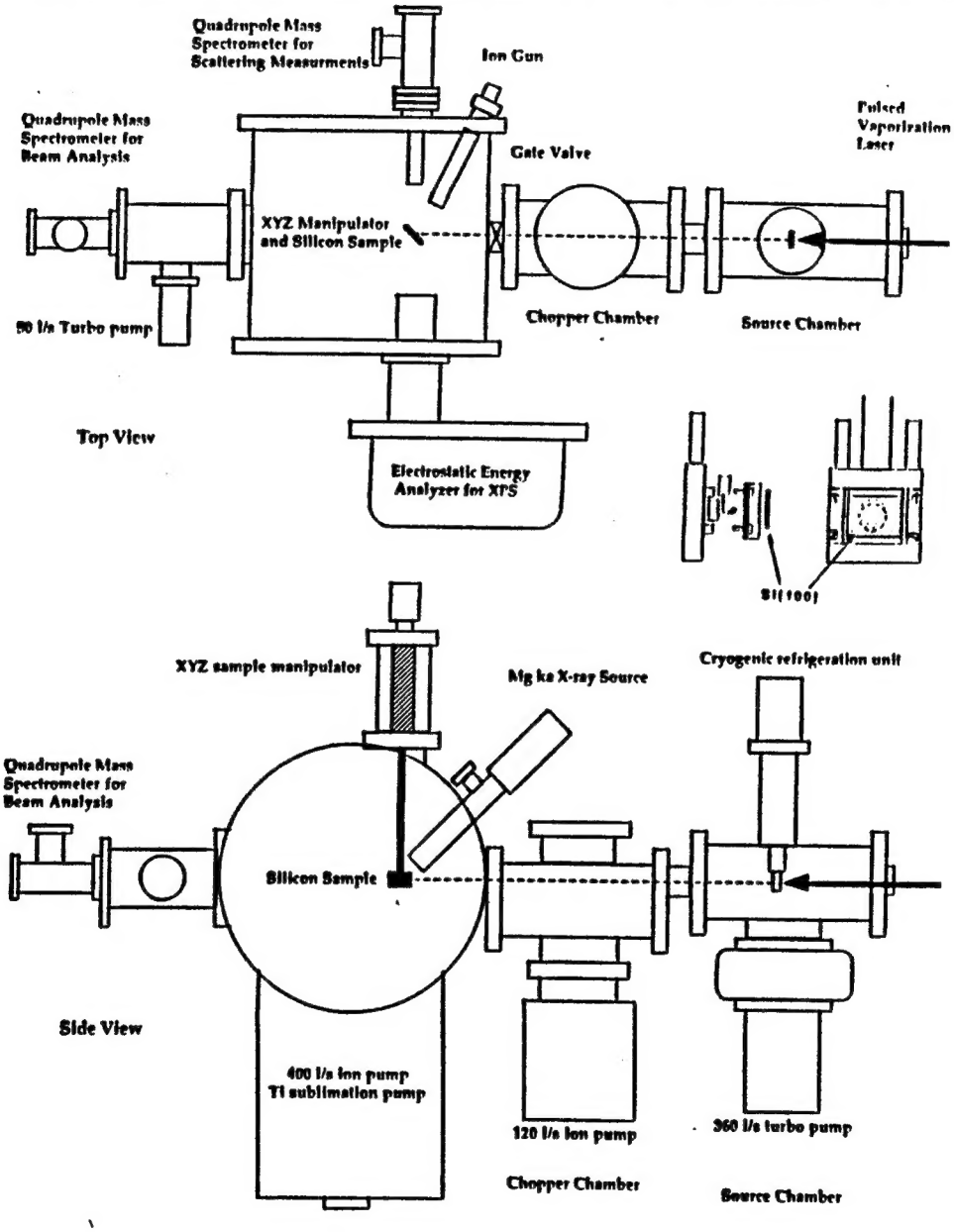


**Fig. 1 Schematic of the semiconductor etching apparatus using the cryogenic laser vaporization beam source.**

and fragments by rapid heating, photodissociation, and hydrodynamic expansion. This works as a reliable source of translationally fast particles for the surface scattering, etching, and deposition experiments which are carried out in the main interaction chamber. Previously we studied the species in the vaporized beam and determined their internal energies (vibration and rotation).[58,59] The general characteristics of the beam are high kinetic energy, low internal energy, and moderate to small amounts of fragmentation. Reliable sources of translationally fast (≈1-5 eV mean) $Cl_2$, F, and Cl have been produced for the etching studies.[1-5]

Figure 2 shows a set of typical kinetic energy profiles for laser vaporization of chlorine molecular films. The mass spectrometer is tuned to $Cl_2$, although a small extent of Cl atoms is also observed. The three different ranges of kinetic energy are obtained by varying the laser power or time between laser pulses; the latter allows varying thicknesses of deposition before vaporization. The translational energy of the ejected particles is analyzed by time-of-flight mass spectrometry using the quadrupole mass spectrometer located on the other side of the interaction chamber. The flight distance is 1.3 m. The average kinetic energies are denoted on the figure. It can be seen that the average energy can be easily varied over a wide range and that the highest kinetic energies (up to 6 eV) are considerably higher than can be achieved by seeded beam techniques.

A chopper, which is synchronized with the laser vaporization pulse, is housed in a small differentially pumped chamber (Fig. 1). The chopper allows a

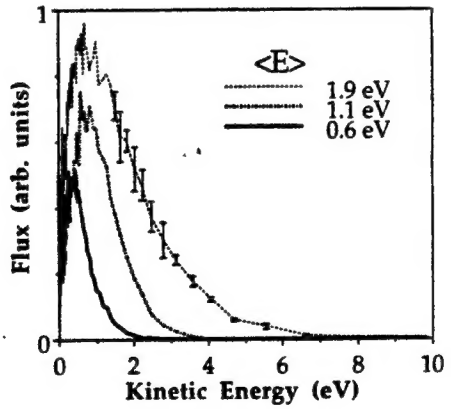


**Fig. 2 Typical time-of-flight kinetic energy distributions for laser vaporization of $Cl_2$. The plots are rescaled to remove overlap.**

narrow slice of the full velocity distribution to be transmitted for kinetic energy-resolved experiments. The results of the chopped beam are described further below.

Because the scattered fluxes for the chopped beam are weak, and since preliminary investigations to observe etch profiles with a scanning electron microscope were not successful, a new source arrangement was constructed to permit higher average fluxes (Fig. 3). It consists of a rotating transparent substrate, so that a fresh region of the cryogenically deposited source material is sampled by each laser vaporization pulse, permitting much higher repetition rates. Whereas we frequently operate at one pulse per second or as low as one pulse per ten seconds, the new source should in principle allow up to 20 pulses per second under routine operation. Thus far this source has not worked as expected because of the difficulty of achieving the very low temperatures needed to condense chlorine through the more massive rotating stage.

The fast beams are directed onto the substrate in the main interaction chamber, which is maintained under ultrahigh vacuum. A mass spectrometer is positioned at right angles to the primary beam to analyze the scattered products of the etching, to obtain sticking coefficients as a function of kinetic energy, and to study the scattering and dissociation of molecules upon collision with the semiconductor substrate. For higher flux studies of phenomenological etching rates

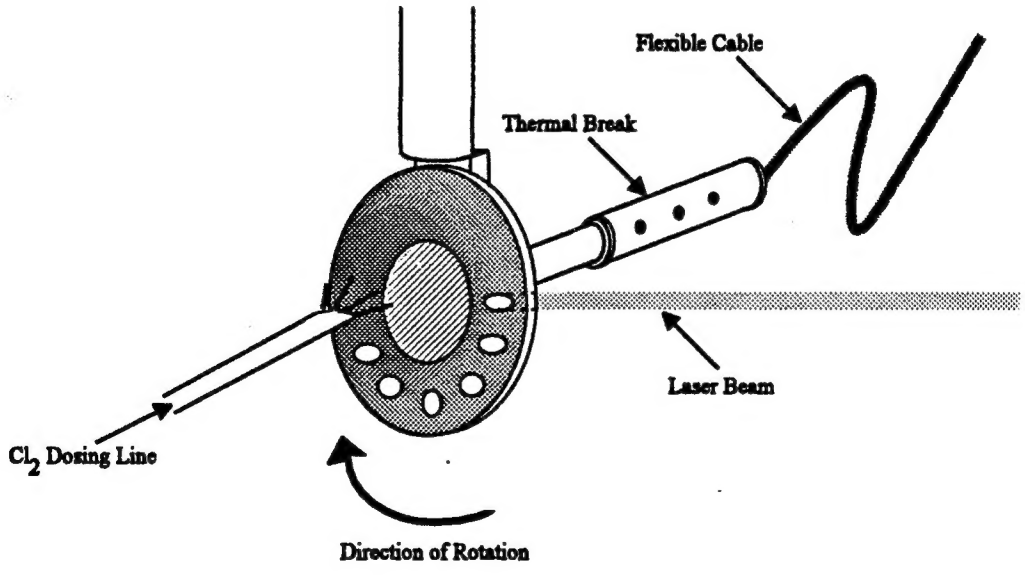


**Fig. 3 High repetition rate laser vaporization source in development.**

or the anisotropies of the etch profiles, the substrate may be positioned closer to the vaporization source. A quartz crystal microbalance may also be used to measure the mass loss or uptake. The time resolved traces of the formation of etching products are a novel part of these studies and represent a powerful diagnostic, which is only possible because of the pulsed nature of the laser vaporization beam source.

## Source Characterization

A portion of the research work is directed towards the development of new sources of reactive atoms and molecules for use in the etching studies. In the sections immediately below, the recent results are descrive to achieve velocity selection, to investigate the generation of atomic sources, and to understand laser vaporization of mixtures of species. First it is valuable to summarize some information about the mechanism of the laser vaporization process. The measurements show that laser vaporization of thin films is a general source of translationally fast neutral species. The process appears to be similar for many different species and for different wavelengths of light used. The laser energy is most likely deposited initially into electronic states of molecules in the solid, but this energy is rapidly released as heat by a variety of intra- and intermolecular relaxation processes. Vibrational, rotational and translational motions of the nuclei result. Some dissociation can occur, but molecules which are caged have a high propensity to recombine. When energy is deposited into the film more rapidly than thermal conduction can remove it, zones of the film become superheated. Molecules at the vacuum interface can evaporate directly with low kinetic energy, but molecules that are temporarily trapped in the bulk can produce a hydrodynamic expansion and shock front, which ejects these molecules with high kinetic energy. During the expansion, collisions can serve to cool the rotational and vibrational states and direct the flow of the expanding gas in the forward direction.

### ICl - An Atomic Cl Source

Numerous studies have indicated that atomic Cl can play an important role in the etching of silicon.[46,60-62] For example, laser assisted etching experiments suggest that gas phase photodissociation of molecular chlorine increases adsorption of Cl atoms on the surface, and this enhances the etching process. Atomic Cl is

undoubtedly an important species in plasma etching, as well. Previously, a source of translationally fast molecular $Cl_2$ was developed, however in that beam it was shown that 7-14% of the species are atomic Cl. Thus, the independent roles of atomic and molecular chlorine species in the etching process are not easily distinguished. To address this issue, a more pure source of atomic Cl was sought, so that the effects of the atomic species could be studied independently.

Intuition from previous studies of laser vaporization of NO, $Cl_2$, and $XeF_2$ suggested that ICl may be a favorable precursor to produce atomic Cl by laser vaporization. The rationale is that the weak bond of ICl would lead to considerable dissociation at the high transient temperatures caused by laser heating of the cryogenic film. A similar effect was observed with $XeF_2$, in which substantial fragmentation to F atoms occurs, whereas with NO, there is no detectable fragmentation. An intermediate case is $Cl_2$, in which only 7-14% of the beam is atomic fragments.

Figure 4 shows the time-of-flight traces for Cl, I and ICl upon laser vaporization of cryogenic films of ICl.[5] In this case, the 532 nm output of the Nd:YAG laser in the green was used, since ICl has an absorption in the visible. In a similar manner observed for $XeF_2$,[3] the ICl is extensively fragmented during the laser vaporization process. There is also some $Cl_2$ and $I_2$ in the vaporized plume, which may arise from disproportionation or recombination of atoms in the source. The figure shows clearly that the Cl atoms have a very different velocity distribution and arrive earlier in time than the I and ICl. This effect has also been observed for $XeF_2$, in which the F atoms arrive earlier in time. It is basically attributed to the lighter mass of F or Cl compared to $XeF_2$ or ICl, which results in a higher velocity for a similar thermal energy content, discussed further below.

Figure 5 shows the arrival times and mean kinetic energies of the Cl atoms in comparison to the I atoms. Although not shown on the figure, the mean energy of the Cl atoms can be tuned from 0.4 to 3.4 eV by varying the conditions of film thickness and laser energy density. The most energetic Cl atoms in the distribution have kinetic energies as high as 8.8 eV. Although the I atoms always arrive later in time, they have substantially more kinetic energy. The mean I atom energies can be varied from 0.7 to 7.5 eV, and the most energetic I atoms have 29 eV. To some extent the heavier species are swept along in the hydrodynamic expansion that

occurs in the laser vaporization process, thus increasing their kinetic energy.

If the ICl is dissociated by the rapid thermal heating, conservation of momentum will constrain the initial Cl atom velocity to be 3.6 times greater than the I atom velocity. Thus, the Cl atoms would contain greater kinetic energy initially. However, in a hydrodynamic or supersonic expansion, the heavier species can be swept along with the velocity of the lighter species by collisions.[63] Thus, the heavier I atoms will undergo collisional energy transfer with the faster Cl atoms, which will equilibrate their velocities in the limit of many collisions. This can be clearly seen in Fig. 5, when long times are used between laser pulses to achieve

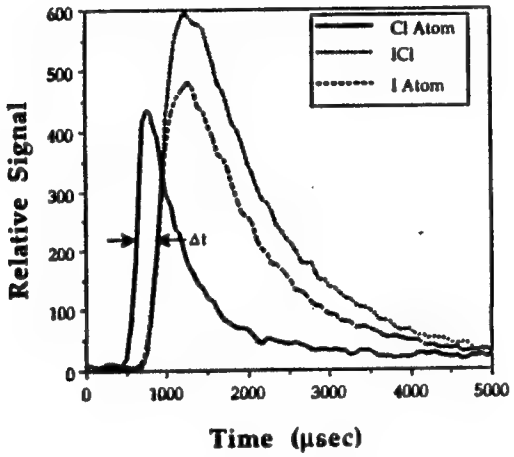


**Fig. 4 Time-of-flight traces for Cl, I, and ICl vaporized from ICl films.**

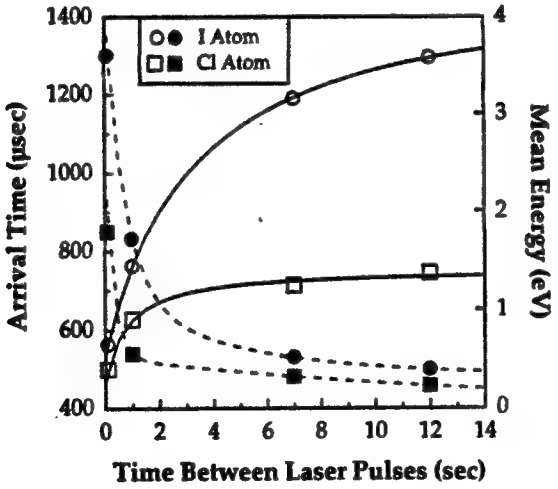


**Fig. 5 ● arrival time of I atoms, ■ arrival time of Cl atoms, ○ mean energy of I atoms, ❑ mean energy of Cl atoms, plotted vs. time between laser pulses, which increases the thickness of the ICl film.**

thicker films of ICl. The velocities of the two species are nearly equal in this collision-dominated case, and the heavier species has the greater kinetic energy. Since Fig. 5 shows that the I atom always has a higher energy than Cl, collisional energy transfer most likely occurs on a time scale faster than the atoms escape from the surface. In the limit of large numbers of collisions, i.e. very thick films, the velocities of Cl and I will approach the same value; in this case our observed ratio of kinetic energies for I/Cl is 3.3, in good agreement with the theoretical limiting value of 3.6 for thermalized atoms.

Figure 4 shows that the laser vaporization conditions can be adjusted so that a portion of the Cl atoms arrive well before the heavier molecules. In the next section we discuss how a mechanical chopper can be used to select this fast portion of the beam, which results in velocity-selected Cl atoms.

**Velocity Selection**

For velocity selection, a light weight, high speed mechanical chopper wheel, 13 cm in diameter, has been fabricated with two slots located 180° apart on the perimeter of the wheel. The direct coupled motor rotates the chopper at ≈400 Hz. A light emitting diode/photodiode trigger is mounted around the slot opening and is used to synchronize the timing for the laser pulse with the opening of the chopper. Thus, a portion of the beam can be transmitted with a variable time delay after the laser pulse. The widths of the slots can also be selected to vary the opening time. Figure 6 shows a typical example for laser vaporization of ICl, in which the chopper is operated to transmit an ≈6 μs slice of the total 5000 μs time-of-flight distribution (compare Figs. 4 and 6).

The chopper was originally designed with two slots opposing each other on the wheel. However, for some time-of-flight distributions, the second opening comes before the molecular pulse has finished. Thus, in Fig. 6, it can be seen that some slow I atoms are transmitted during the second opening of the chopper as the low velocity tail of the vaporization pulse passes through. The second opening of the chopper will be eliminated by constructing a chopper with only a single slot in 360° and counterbalancing the wheel at a different radius to account for the cutaway portion. Figure 6 shows that during the first chopper opening both Cl and $Cl_2$ are transmitted. In this particular run, contamination from $Cl_2$ occurred in the ICl

sample. The extent of $Cl_2$ depends on the purity of the ICl and cleanliness of the system and can be reduced to a more negligible amount.

The chopper is mounted near the laser vaporization source. The group of velocities that is transmitted by the chopper has some initial spread which broadens somewhat more (≈20-40 μs for Cl) during the flight distance to the analysis quadrupole. Nevertheless, quite narrow slices from the full kinetic energy

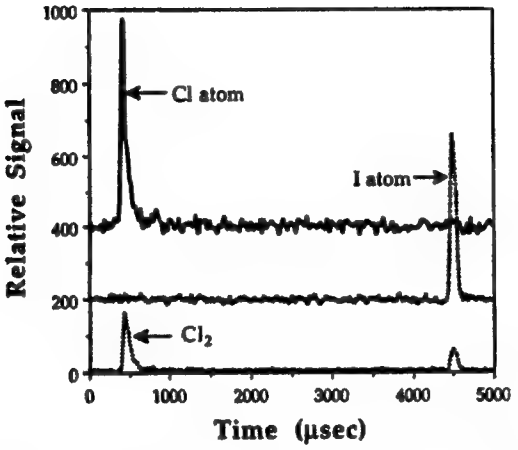


**Fig. 6 Time-of-flight of arrival for the chopped velocity distribution.**

distribution are achieved. The spread of kinetic energies is decreased by more than a factor of ten, which will be a powerful tool for energy-resolved studies of etching. Since the fluxes from the chopped source are considerably reduced, as already noted above, it will be important to implement the high repetition rate source of Fig. 3 to make reliable measurements.

**Laser Vaporization of Mixtures of Condensed Species**

Laser vaporization of mixed materials is technologically important for fields such as matrix-assisted, laser desorption mass spectrometry. An interesting problem arises when one of the components is strongly absorbing, while the other is transparent to the laser. For very thin films, the transparent material can only be ejected if there is energy transfer between molecules on the surface. In thick films, the transparent material can be entrained by the vaporization of the absorbing compound. Because the energy transfer mechanisms and cooperative behavior of mixed systems are in need of further detailed study, we selected a simple chemical

system for further investigation. In our studies, we form mixtures of Xe with $Cl_2$ and vaporize them with the 355 nm output of a Nd:YAG laser. In this case, only the chlorine is absorbing, and the Xe is completely transparent. The only chemistry that can occur is the dissociation of $Cl_2$ to Cl. All of our films are relatively thick, so explosive vaporization occurs, resulting in entrainment of the Xe species by the ejecting material. It is assumed that both $Cl_2$ and Xe stick with similar probabilities on the 20 K substrate.

Figure 7 shows an example of the time-of-flight (TOF) data for Xe and $Cl_2$ at two different initial mixture ratios, (90% Xe/10% $Cl_2$ and 50% Xe/50% $Cl_2$).[4] For the 50/50 mixture, it can be seen in the figure that the $Cl_2$ and Xe have almost identical time-of-flights. The Xe is entrained by the vaporizing chlorine with only a small

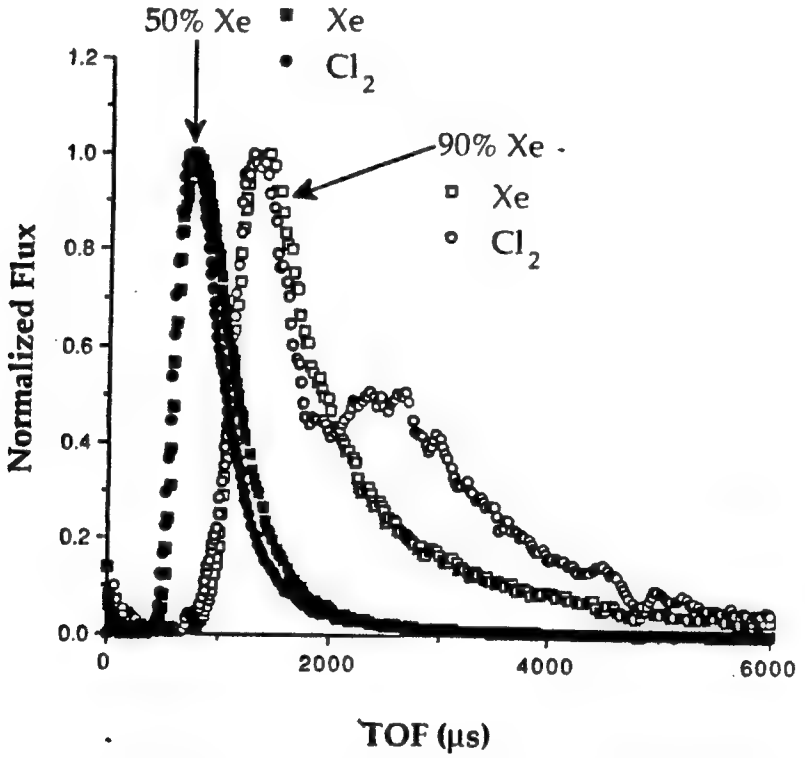


**Fig. 7 time-of-flight traces for Xe and $Cl_2$ from laser-vaporized mixtures.**

velocity slip. Of course, the resulting kinetic energy of the Xe is greater than $Cl_2$ because of the difference in masses. At 90% Xe, however, the time-of-flight distributions of $Cl_2$ and Xe are substantially different. First the overall time of arrival of both Xe and $Cl_2$ is much later, which is reasonable because the amount of absorbing material has been greatly decreased, and thus less energy is deposited in

the film. However, the Xe TOF follows only the fast component of the $Cl_2$, and a pronounced slow component of $Cl_2$ is observed without a simultaneous Xe peak.

The presence of two velocity components in the vaporized $Cl_2$ suggests that the cryogenic film may be inhomogeneous. A possible explanation is that some of the chlorine molecules aggregate, so that there are regions of relatively high chlorine concentration in the condensed film. The more energetic part of the beam can be associated with the concentrated regions, while the slower part of the beam corresponds to chlorine molecules that are dilutely dispersed throughout the Xe. The data for the two velocity peaks have been successfully fit with separate temperatures and stream velocities.

Another interesting result of the studies on mixtures pertains to the ratio of $Cl : Cl_2$ at different times during the time-of-flight transient. Figure 8 displays some of this data, taken from a mixture of 90% Xe/10% $Cl_2$. Here, the portion of the $Cl_2$ that is merely cracked to $Cl^+$ in the mass spectrometer has been subtracted out and the signals normalized for the ionization efficiencies. The figure shows clearly that a higher percentage of Cl atoms is produced in the high velocity subgroup of the vaporization. The presence of Cl atoms only in the fast portion of the beam implies

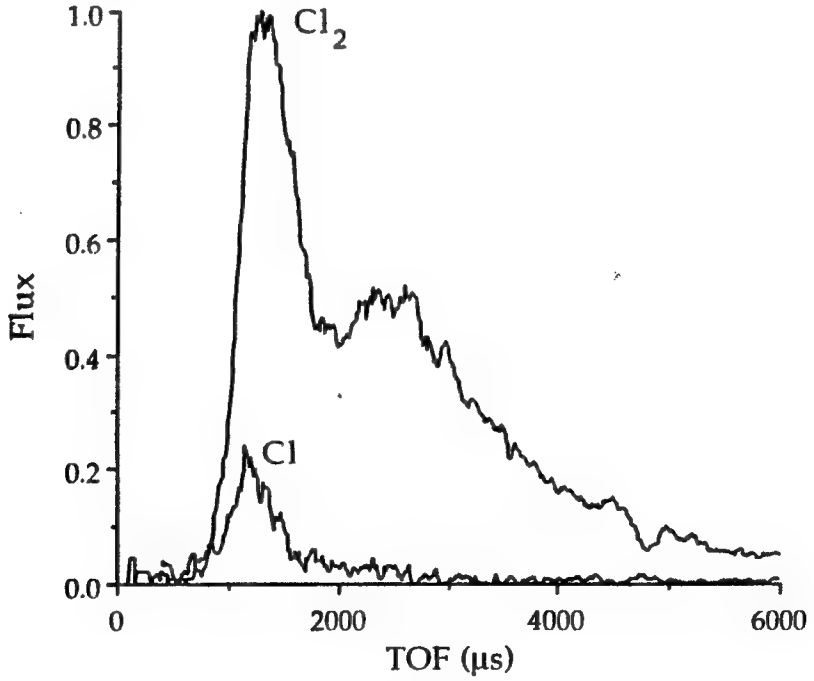


**Fig. 8 Normalized time-of-flight distributions for Cl and $Cl_2$ after correction for mass spectral cracking.**

that this part of the beam originates in a relatively hot region of the film. The absence of Cl atoms in the slow part of the beam is consistent with reports that when $Cl_2$ is embedded in a Xe matrix, the molecule experiences an almost perfect caging effect which prevents dissociation.[64]

The studies of $Xe/Cl_2$ mixtures provide insight into the laser vaporization of transparent materials and the development of molecular beam sources of these species. In the case of matrix-assisted laser desorption, the principles of mixed systems are already being used to advantage. Our results suggest that aggregation and homogeneity of the film are important parameters to be considered to optimize the desired process.

**Enhanced Etching of Single Crystal Si by 1-6 eV Chlorine**

In this work, the effect of chlorine translational energy on the silicon (100) - chlorine etching reaction is investigated.[6,7] The pulsed laser vaporization source is arranged in the configuration shown in Fig. 1 on page 8, and $SiCl_x$ products are detected by a mass spectrometer in the specular direction (90° from the incoming beam while the Si wafer is inserted at 45° to the incident beam). All of the results are normalized for the measured incoming flux of particles, so that data from different kinetic energy conditions are directly comparable. P-type doped Si(100) is used in these studies (resistivity 10-25 Ω-cm).

Room temperature p-type silicon typically does not undergo sustained etching by dosing with thermal chlorine,[45,47,65-68] and this is confirmed here by studies with a pulsed valve to introduce the chlorine. The most significant result of this work is that sustained $SiCl_x$ product formation (etching) occurs for room temperature single crystal silicon when using chlorine beams with 1-6 eV kinetic energy; we also find that the etching rate is accelerated dramatically by increasing the kinetic energy.

Careful characterization of the hyperthermal beam source indicates that ≤7% of the species in the beam is atomic Cl. In contrast to the studies above on mixtures of $Xe/Cl_2$, in this case the Cl atom percentage was relatively insensitive to the laser vaporization conditions. The evidence suggests that the increased kinetic energy of the chlorine molecules is an important factor in the enhanced etching; Szabo, Farrall and Engel have indicated from recent experiments in their laboratory that Cl atoms may be a necessary component to form the chlorinated layers.[69] We are

pursuing additional studies to determine the effect of etching by atomic Cl as well. Below, we describe the initial results of the kinetic energy experiments in more detail.

**Products of the Etching**

A wide range of hyperthermal kinetic energies are produced by the laser vaporization process. In these experiments, the full beam from the laser vaporization process was used in order to maximize the signals; thus the variation in velocity was accomplished broadly by changing the laser vaporization conditions. We studied etching of Si(100) with beams having mean kinetic energies of 0.4, 0.6, 0.8, 1.1, 1.8, 1.9, and 2.0 eV. The velocity distributions are relatively broad, and Fig. 2 on page 9 shows a good example of the distributions of energies for three of the beams used in this study; the beams depicted in the figure have mean kinetic energies of 0.6, 1.1, and 1.9 eV. From the figure it is evident that the beam with 1.9 eV mean energy has a substantial fraction of chlorine molecules with energy above 3 eV, while the other two beams have almost no molecules above 3 eV energy. Similar limits distinguish the broad ranges of kinetic energies incident on the Si(100) sample.

The silicon sample is first cleaned and annealed and then subjected to the incident hyperthermal pulsed beam of molecules. The characteristic signature of the etching process is the detection of pulses of $SiCl_3^+$ in the mass spectrometer (Fig. 9). In contrast to other studies which find predominantly $SiCl_2$,[70-74] and sometimes $SiCl_4$, the $SiCl_3$ product is the largest in these investigations (observed ratio 4.5 : 1 for $SiCl_3^+$ : $SiCl_4^+$ with a measured cracking ratio for $SiCl_4$ to produce $SiCl_3^+$ : $SiCl_4^+$ of 1.8 : 1). The $SiCl_3^+$ ion peak amounts to an $8 \times 10^{-4}$ fraction compared to the scattered $Cl_2^+$ peak.

In the studies in this laboratory, the $SiCl_3$ product is found to be a predominant species formed in the kinetic energy enhanced etching, even after correction for the mass spectral cracking of $SiCl_4$. Careful cracking patterns were measured for a pure sample of $SiCl_4$ with the mass spectrometer, and the extent of $SiCl_4$ product does not account for the whole $SiCl_3^+$ signal. In Fig. 10, the $SiCl_3^+$ amplitude has already been corrected for the extent of cracking of $SiCl_4$ by the mass

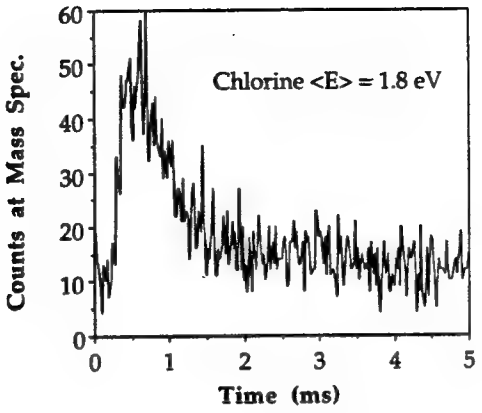


**Fig. 9 Detected pulse of $SiCl_3^+$ resulting from hyperthermal beam etching.**

spectrometer ionizer. It is possible that vibrationally excited $SiCl_4$ is produced in the etching and that this species has a very different cracking pattern, however the trends observed with substrate temperature also suggest that $SiCl_3$ formation may occur directly at room temperature with the hyperthermal beam. From Fig. 10, it can be seen that the relative product "distribution" shifts from $SiCl_3$ and $SiCl_4$ to

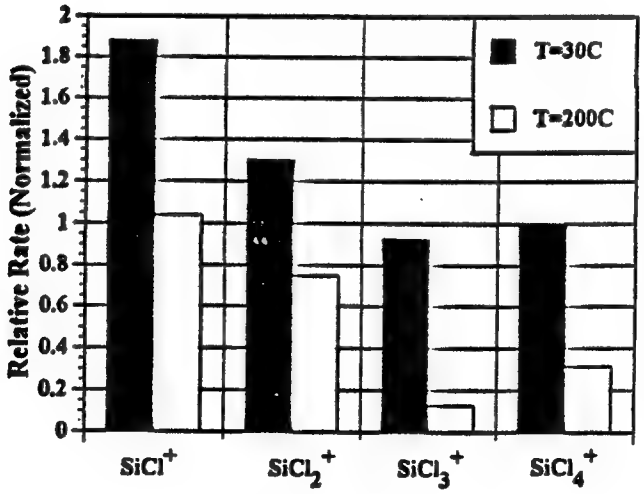


**Fig. 10 Product distributions from kinetic-energy-enhanced etching.**

SiCl and $SiCl_2$ as the substrate temperature is increased from 30° C to 200° C. Note that the total quantity of etch products actually decreases with increasing temperature, most likely because the surface coverage of chlorine is reduced at the higher temperatures.

The formation of a direct $SiCl_3$ product is not customary but may be a result of the higher kinetic energy neutral bombardment. In collaboration with H. Feil at Philips in the Netherlands, a mechanism has been observed in large scale molecular dynamics calculations which releases an $SiCl_3$ directly. In these calculations the $Cl_2$ incident energy is 10 eV, and the slow step in the formation process is the production of a top site $SiCl_3$ from $SiCl_2$ on the surface. Then the release of $SiCl_3$ occurs by a nearby impact of the enhanced kinetic energy $Cl_2$. Supporting evidence for this mechanism comes from experiments on the observed time of arrival of the $SiCl_3$ product. The first $SiCl_3$ molecules to arrive have a kinetic energy of ›0.5 eV, suggesting a highly nonthermal ejection process. Figure 10 also shows that the traditional mechanism of thermal desorption of $SiCl_2$ may become more predominant at increased substrate temperatures, thus indicating a change in the mechanism with substrate temperature.

An important result of the experiments comes from a measurement of the arrival time of the $SiCl_3$ species at the mass spectrometer. Assuming the earliest possible arrival time of $Cl_2$ at the silicon surface (6 eV), the earliest portion of the $SiCl_3$ signal has 0.57 eV of kinetic energy. Since the thermal energy of the surface is far below this value (2kT = 0.055 eV), the mechanism for production of $SiCl_3$ must involve a highly energetic release, for example when the fragment is formed with substantial excess energy. It will be important to verify this energetic release by further theoretical calculations.

**XPS Measurements of Chlorine Uptake on Si(100)**

Since the hyperthermal beam pulses contain less than 0.1 monolayer of chlorine flux each, the first few pulses produce no observable silicon chloride products. Etching is observed promptly upon exposure to the hyperthermal beam whenever the silicon is first precovered with chlorine. The onset of etching is correlated with the initial chlorine precoverage by x-ray photoelectron spectroscopy (XPS) measurements of the chlorine 2p feature. Figure 11 shows a typical set of XPS

data for different mean kinetic energies of the hyperthermal beam. The horizontal axis is indicated directly in terms of the number of beam pulses. A break in the slope of the chlorine XPS signal is seen at 200 pulses, at essentially all energies. This suggests that the most easily occupied surface sites, presumably dangling bond or defect sites, are essentially saturated with chlorine at this exposure. The adsorption of additional chlorine is more difficult because it requires breaking Si-Si bonds, and this is precisely where the onset of etch products is observed, along with a change in the rate of the coverage.

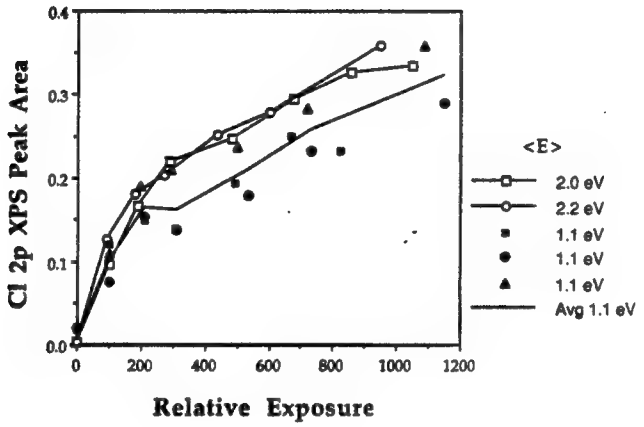


**Fig. 11 XPS signal from Cl 2p following exposure at different energies.**

**Energy Dependence of Etching Rate**

Figure 12 shows the total $SiCl_3^+$ etch product signal as a function of exposure, again denoted by the number of incident beam pulses, using the same horizontal calibration as Fig. 11. The figure shows the results for several different mean kinetic energies of the incident $Cl_2$. The exposures are normalized for fluctuations in the beam flux. The slopes of the plots correspond directly to relative etching rates. At low $Cl_2$ exposures, all of the data have a similar slope, which corresponds to the initial precoverage regime. The similarity of the etching rates at low exposure shows that certain minimum conditions of chlorine coverage and surface erosion are necessary for the etching. At higher exposures, three distinctly different slopes, or etch rates, are detected.

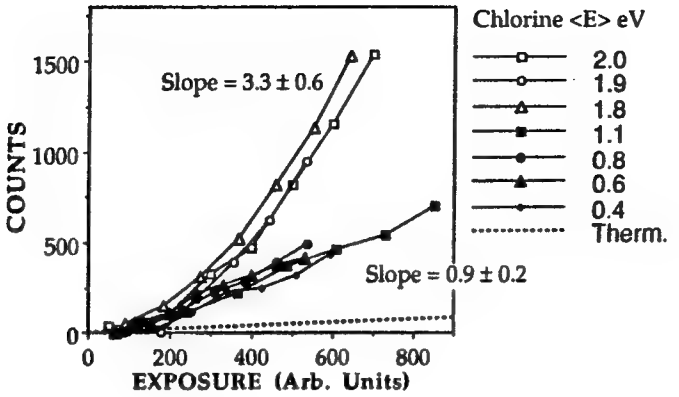


**Fig. 12 Total etch product ($SiCl_3^+$) as a function of exposure and energy.**

The dotted line corresponds to the results with a thermal source of chlorine from a pulsed molecular beam valve. No etching is detected at all, and the slight positive slope is drawn to account for the maximum error bars determined from the signal-to-noise ratio. A second group of kinetic energies have a slope of 0.9 on the graph; this data corresponds to the beams with mean kinetic energies of 0.4, 0.6, 0.8 and 1.1 eV incident $Cl_2$. The highest slope of 3.3 corresponds to the group of beams with mean kinetic energies of 1.8, 1.9. and 2.0 eV. The maximum etch rate with the highest kinetic energy of $Cl_2$ is >30 times faster than the limit of the etch rate observed with thermal $Cl_2$. In addition, the etch rate increases by a factor of 3.6 from the group of kinetic energies with mean energies between 0.4 -1.1 eV to the group with mean energies between 1.8-2.0 eV.

The factor of 3.6 change in etch rate suggests the possible existence of an energetic threshold, which can be overcome by translational energies in the range of 3-6 eV. This is the range of energies that are absent in the beams with mean kinetic energies between 0.4-1.1 eV. The difference between the thermal result and the results for all of the hyperthermal beams suggests the possible existence of another energetic threshold. However, this could also be due to the small percentage of Cl atoms in the hyperthermal beams. If ≈3 eV is an important energetic limit, it is

worth noting that this is just slightly higher than the Si-Si bond energy of 2.3 eV. This corroborates the theoretical calculations in which the difficult step is to break a Si bond to the bulk. The results suggest that the direct utilization of gas phase kinetic energy to break surface bonds is feasible and may play an important role in dry etching processes with plasma sources.

**Uptake of Chlorine by Amorphous Silicon**

During the course of this work, the uptake of chlorine in the hyperthermal beams by amorphous silicon was also studied, using a quartz crystal microbalance. This technique has been pioneered by Winters[50] and Coburn and Winters.[54,65] A quartz sample is cut thinner than the frequency of the microbalance, and then about 20,000 layers of amorphous silicon are deposited on top. The removal or uptake of material is sensed by the change in resonant frequency of the microbalance. While the initial precoverage was similar to the XPS results for single crystal silicon, we found that a rapid uptake of chlorine continued essentially indefinitely on amorphous silicon. This indicates that a much deeper corrosion layer of chlorinated silicon forms on the amorphous silicon, compared to single crystal silicon. Since these results differ significantly from the single crystal silicon behavior, we do not believe that the amorphous silicon results are a good model for the single crystal etching.

**Sticking and Scattering of Hyperthermal $Cl_2$ and Cl with Si(100)**

The basic aspects of scattering and uptake of hyperthermal chlorine molecules by Si(100) have been studied recently by several research groups.[6,75-80] Using seeded supersonic sources and heated nozzles, many measurements have been reported for $Cl_2$ kinetic energies up to 0.7-1.5 eV. A novel aspect of the studies reported here[77] is that higher kinetic energies can be achieved with the laser vaporization beam source. If further improvements can be made to the beam flux in this source, it may be possible to extend the measurements of scattering probabilities and etch rates to as high as 8-10 eV.

In the scattering experiments performed with the laser vaporization source,[77] the velocity-selected pulsed beam is scattered by Si(100) and in separate experiments,

the same beam is scattered by quartz, which is used a reference. This assumes that the quartz is noninteracting with the $Cl_2$; from measurements performed over a long period of time, this appears to be a correct assumption. The specular scattering direction is detected with the quadrupole mass spectrometer, and time histories of the scattering intensity are acquired.

The molecules of $Cl_2$ that are scattered by Si(100) have a time-of-arrival and time duration that mimic identically the incoming beam pulse time profile and velocity, indicating that the scattered species are essentially elastically scattered. However, the scattering by quartz leads to a substantial broadening of the scattered pulse in time to longer delays, suggesting that energy is lost, most likely by multiple collisions or efficient transfer of energy to the substrate. In addition, the scattering by Si(100) shows a very sharp specular peak on top of a broad angular distribution of scattered molecules; however the quartz scattering exhibits only a broad angular distribution. The sharp specular scattered molecules from Si represent only a very small fraction of the total scattered flux, and this feature may be indicative of a unique repulsive scattering mechanism that might not be occur at lower kinetic energies. Since most of the data was taken at the specular angle to achieve maximum signal-to-noise, the amplitudes from the Si scattering are corrected to obtain the total scattering flux.

The percent scattered fluxes of $Cl_2$ from Si(100) are shown in Fig. 13 for four different velocity-selected incident beam energies (0.6 eV, 0.71 eV, 1.3 eV, and 2.59 eV). There is less scattered flux with increasing incident energy, indicating that for clean Si(100) the rate of uptake (chemisorption or reaction) is enhanced with increasing kinetic energy. The incident kinetic energy may supply the necessary activation energy for dissociative chemisorption, for example. The figure also indicates how the scattered flux varies with exposure of the surface to the number of beam pulses. At each beam energy, the scattered flux increases as the coverage of chlorine on the surface increases. In these experiments, the coverage is increased more rapidly between measurements by exposing the substrate to the higher flux, unchopped beam. In separate experiments, the coverage is calibrated by Auger measurements and corresponds to approximately 12% of a monolayer (ML) at 1000 pulses. The rate of coverage starts out fast and decreases with increasing number of pulses, presumably as dangling bond sites become occupied. It is also possible that

$SiCl_x$ products begin to be formed, as will be discussed further in the etching section below.

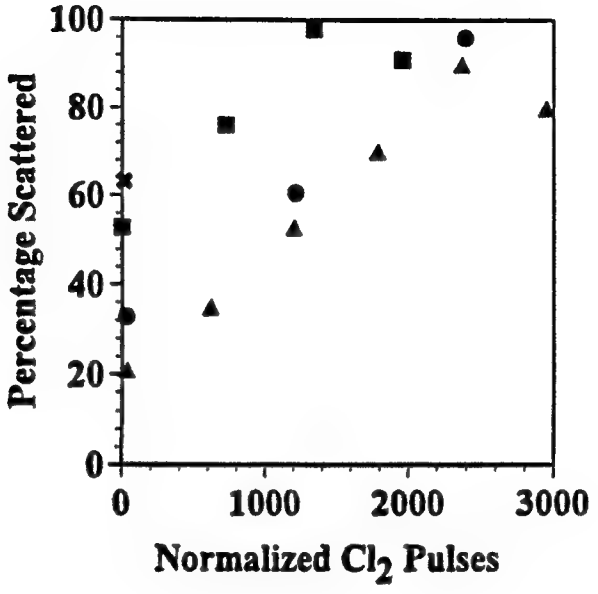


**Fig. 13 Percentage of scattered $Cl_2$ as a function of incident beam energy. (✖) <E> = 0.6 eV. (■) <E> = 0.71 eV. (●) <E> = 1.3 eV. (▲) <E> = 2.59 eV. Increased exposure with number of pulses of the unchopped beam indicate that the percent scattered increases with coverage.**

A multiplicity of processes can occur in the scattering experiments described above. For example, the incident $Cl_2$ can be dissociatively chemisorbed, producing two Cl atoms bound to the surface; one Cl atom can be adsorbed while one Cl atom is released into the gas phase; $SiCl_x$ etch products can be formed and released into the gas phase; the incident $Cl_2$ molecule can be scattered in tact; two Cl atoms can be scattered. There is no evidence in these experiments that additional Cl atoms are produced, however $SiCl_x$ products are observed after the initially clean surface becomes chlorinated. In measuring the scattered $Cl_2$ molecules, it is presumptuous to attribute the difference between the fluxes scattered from Si and quartz to the amount that has chemisorbed. However, related experiments to measure surface coverage with the Auger provide corroborating evidence that a large fraction of the $Cl_2$ that is not scattered becomes chemisorbed.

For comparison to other reports, it is therefore valuable to derive an upper limit for the initial sticking probability ($S_0$) from our measurements.[77] These results are shown in Fig. 14. The upper limit for $S_0$ varies from about 25% at 0.5 eV to over 80% at 2.7 eV. These limits are for a 45° incident beam. For comparison to other measurements at normal incidence, it may be necessary to scale the results for the energy normal to the surface. For example, in the study of Sullivan *et al*[78] the initial sticking probability at 0.6 eV is 76% (normal incidence), while at 0.85 eV (45° incidence in our work) the comparable $S_0$ would be 48%. The lack of agreement

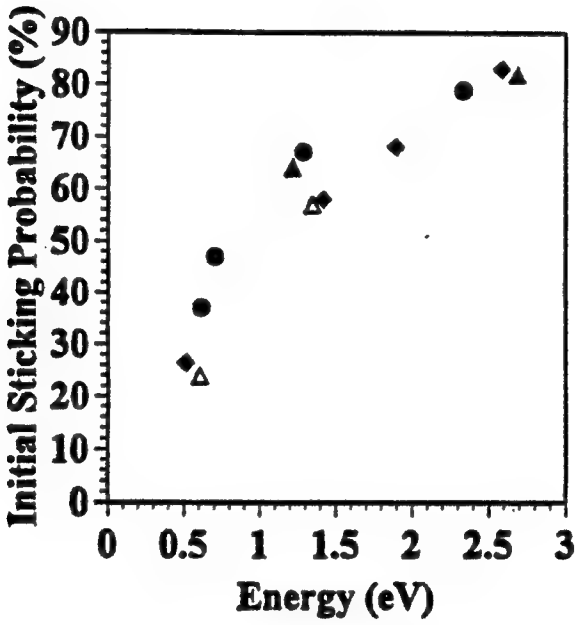


**Fig. 14 Upper limit of $Cl_2$ and Cl sticking probabilities ($S_0$) vs. kinetic energy. (●) and (◆) Two different runs using velocity-selected kinetic energies of $Cl_2$ . (▲) Two different average energies using the full kinetic energy distribution of $Cl_2$ (not velocity selected). (Δ) Two different average energies of Cl atom using the full kinetic energy distribution (not velocity selected).**

between the absolute values is mainly at lower energies, and the general trend of increased sticking with increasing energy is in reasonable accord between the two studies. However, both studies differ from the trend with energy reported by Geuzebroek *et al*.[79]

## References


1. L. M. Cousins and S. R. Leone, J. Materials Res. **3**, 1158 (1988).

2. L. M. Cousins and S. R. Leone, Chem. Phys. Lett. **155**, 162 (1989).

3. R. Levis, C. J. Waltman, L. M. Cousins, R. G. Copeland, and S. R. Leone, J. Vac. Sci. Technol. **A8**, 3118 (1990).

4. F. X. Campos, C. J. Waltman, and S. R. Leone, Chem. Phys. Lett. **201**, 399 (1993).

5. G. C. Weaver, F. X. Campos, and S. R. Leone, Mat. Res. Symp. Proc. **285**, 249 (1993).

6. F. X. Campos, G. C. Weaver, C. J. Waltman, and S. R. Leone, Mat. Res. Symp. Proc. **236**, 177 (1992).

7. F. X. Campos, G. C. Weaver, C. J. Waltman, and S. R. Leone, J. Vac. Sci. Technol. B **10**, 2217 (1992).

8. T. Nakano, N. Sadeghi, and R. A. Gottscho, Appl. Phys. Lett. **58**, 458 (1991).

9. G. King, F. C. Sze, P. Mak, T. A. Grotjohn, and J. Asmussen, J. Vac. Sci. Technol. A **10**, 1265 (1992).

10. T. J. Sommerer and M. J. Kushner, J. Appl. Phys. **70**, 1240 (1991).

11. B. Shizgal and A. S. Clarke, Chem. Phys. **166**, 317 (1992).

12. L. P. Levine, J. F. Ready, and E. Bernal G., J. Appl. Phys. **38**, 331 (1967).

13. J. F. Friichtenicht, Rev. Sci. Instrum. **45**, 1 (1974).

14. S. P. Tang, N. G. Utterback, and J. F. Friichtenicht, J. Chem. Phys. **64**, 3833 (1976).

15. B. G. Wicke, S. P. Tang, and J. F. Friichtenicht, Chem. Phys. Lett. **53**, 304 (1978).

16. B. G. Wicke, N. G. Utterback, S. P. Tang, and J. F. Friichtenicht, Rev. Sci. Instrum. **5**, 151 (1980).

17. B. G. Wicke, J. Chem. Phys. **78**, 6036 (1983).

18. T. Baller, D. J. Oostra, A.E. deVries, and G. N. A. van Veen, J. Appl. Phys. **60**, 2321 (1986).

19. G. N. A. van Veen, T. Baller, and A. E. deVries, J. Appl. Phys. **60**, 3747 (1986).

20. R.W. Dreyfus, R. Kelly, and R. E. Walkup, Appl. Phys. Lett. **49**, 1479 (1986).

21. E. Sutcliffe and R. Srinivasan, J. Appl. Phys. **60**, 3315 (1986), R. Srinivasan, Science, **234**, 559 (1986), R. Srinivasan and A. P. Ghosh, Chem. Phys. Lett. **143**, 546 (1988).

22. F. Engelke, J. H. Hahn, W. Henke, and R. N. Zare, Anal. Chem. **59**, 909 (1987).

23. R. Tembreull and D. M. Lubman, Anal. Chem. **59**, 1082 (1987).

24. M. Salehpour, I. Perera, J. Kjellberg, A. Hedin, M. A. Islamian, P. Håkansson, and B. U. R. Sundqvist, Rapid Comm. Mass Spectrom. **3**, 259 (1989).

25. R. J. Levis and L. J. Romano, J. Am. Chem. Soc. **113**, 7802, 9665 (1991).

26. K. Domen and T. J. Chuang, Phys. Rev. Lett. **59**, 1484 (1987), K. Domen and T. J. Chuang, J. Chem. Phys. **90**, 3318, 3332 (1989).

27. I. Harrison, J. C. Polanyi, and P. A. Young, J. Chem. Phys. **89**, 1498 (1988).

28. N. Nishi, H. Shinohara, and T. Okuyama, J. Chem. Phys. **80**, 3898 (1984).

29. D. E. Brinza, D. R. Coulter, R. H. Liang, and A. Gupta, in "Proceedings of the NASA Workshop on Atomic Oxygen Effects," edited by D. E. Brinza (JPL, Pasadena, CA, 1987).

31. F. L. Tabares, E. P. Marsh, G. A. Bach, and J. P. Cowin, J. Chem. Phys. **86**, 738 (1987).

32. J. E. Rothenberg and R. Kelly, Nucl. Instrum. Methods, **B1**, 291 (1984).

33. M. Eyett and D. Bäuerle, Appl. Phys. Lett. **51**, 2054 (1988).

34. R. A. Powell, ed. "Dry etching for microelectronics" (Elsevier, Amsterdam, 1984).

35. J. Vac. Sci. Technol. **B5** (1987), Proceedings of the 30th International Symposium on Electron, Ion, and Photon Beams.

36. T. J. Chuang, in "Interfaces Under Laser Irradiation," edited by L. D. Laude, D. Bäuerle, and M. Waatelef (Nijhoft, Dordrecht, 1987), p. 235.

37. T. J. Chuang, in "Laser Microfabrication; Thin Film Processes and Lithography," edited by D. J. Ehrlich and J. Y. Tsao (Academic, 1989) p. 1.

38. D. Bäuerle, "Chemical Processing with Lasers," Springer Series in Materials Science (Springer, Berlin, 1986).

39. D. M. Mattox, J. Vac. Sci. Technol. **A7**, 1105 (1989).

40. Technical Support Package for "Energetic Atoms Would Etch Photoresists Anisotropically," NASA Tech Briefs, MSC-21631.

41. I. P. Herman, Chem. Rev. **89**, 1323 (1989).

42. D. L. Flamm and G. K. Herb, in "Plasma Etching: An Introduction," edited by D. M. Manos and D. L. Flamm (Academic, 1989), p. 1.

43. D. L. Flamm, in "Plasma Etching: An Introduction," edited by D. M. Manos and D. L. Flamm (Academic, 1989), p. 91.

44. R. Rossen and H. Sawin, J. Vac. Sci. Technol. A **5**, 1595 (1987).

45. M. C. Chuang and J. W. Coburn, J. Vac. Sci. Technol. A **8**, 1969 (1990).

46. A. Manenschijn, E. van der Drift, G. C. A. M. Janssen, and S. Radelaar, J. Appl. Phys. **69**, 7996 (1991).

47. Z. Walker and E. A. Ogryzlo, J. Appl. Phys. **69**, 548 (1991).

48. K. Suzuki, S. Hiraoka, and S. Nishimatsu, J. Appl. Phys. **64**, 3697 (1988).

49. J. Boulmer, B. Bourguignon, J. P. Budin, and D. Debarre, Appl. Surf. Sci. **43**, 424 (1989).

50. H. F. Winters, J. Vac. Sci. Technol. **A3**, 700 (1985); J. Vac. Sci. Technol. **B3**, 9 (1985).

51. R. A. Powell and D. F. Downey in "Dry Etching for Microelectronics," edited by R. A. Powell, (Elsevier, Amsterdam, 1984) p. 113.

52. R. E. Behringer, P. M. Mankiewich, and R. E. Howard, J. Vac. Sci. Technol. **B5**, 326 (1987).

53. R. Sellamuthu, J. Barkanic, and R. Jaccodine, J. Vac. Sci. Technol. **B5**, 342 (1987).

54. J. W. Coburn and H. F. Winters, J. Vac. Sci. Technol. **16**, 391 (1979).

55. K. Suzuki, K. Ninomiya, S. Nishimatsu, and 0. Okada, Jap. J. Appl. Phys. **25**, L373 (1986).

56. M. W. Geis, N. N, Efremow, S. W. Pang, and A. C. Anderson, J. Vac. Sci. Technol. **B5**, 363 (1987).

57. B. J. Garrison, M. T. Mitchell, and D. W. Brenner, Chem. Phys. Lett. **146**, 553 (1988).

58. L. M. Cousins, R. J. Levis, and S. R. Leone, J. Phys. Chem. **93**, 5323 (1989).

59. L. M. Cousins, R. J. Levis, and S. R. Leone, J. Chem. Phys. **91**, 5731 (1989).

60. Y. L. Li, Q. K. Zheng, Z. K. Jin, M. Yu, Z. K. Wu, Q. Z. Qin, J. Phys. Chem. **93**, 5531 (1989).

61. H. Okano, Y. Horiike, and M. Sekine, Jap. J. Appl. Phys. **24**, 68 (1985).

62. W. Sesselmann, E. Hudeczek, and F. Bachman, J. Vac. Sci. Technol. b **7**, 1284 (1989).

63. D. R. Miller, in "Atomic and Molecular Beam Methods," Vol 1, ed. by G. Scoles (Oxford Univ. Press, New York, 1988), p. 14.

64. M. E. Fajardo, R. Withnall, J. Feld, F. Okada, W. Lawrence, L. Wiedeman, and V. A. Apkarian, Laser Chem. **9**, 1 (1988).

65. J. W. Coburn and H. F. Winters, J. Appl. Phys. **50**, 3189 (1979).

66. R. Kullmer and D. Bauerle, Appl. Phys. A **47**, 377 (1988).

67. E. A. Ogryzlo, D. L.Flamm, D. E. Ibbotson, and J. A, Mucha, J. Appl. Phys. **64**, 6510 (1988).

68. M. Seel and P. S. Bagus, Phys. Rev. B **28**, 2023 (1983).

69. A. Szabo, P. Farrall, and T. Engel, private communication.

70. M. A. Mendicino and E. G. Seebauer, Appl. Surf. Sci. **68**, 285 (1993).

71. J. Matsuo, F. Yannick, and K. Karahashi, Surf. Sci. **283**, 52 (1993).

72. K. Karahashi, J. Matsuo, and S. Hijiya, Appl. Surf. sci. **60/61**, 126 (1992).

73. Q. Gao, C. C. Cheng, P. J. Chen, W. J. Choyke, and J. T. Yates, Jr. J. Chem. Phys. **98**, 8308 (1993).

74. P. Gupta, P. A. Coon, B. G. Koehler, and S. M. George, Surf. Sci. **249**, 92 (1991).

75. A. Szabo, P. D. Farrall, and T. Engel, "Thermal and Direct Etching Mechanisms of Si(100) with a hyperthermal Chlorine Beam," J. Appl. Phys. (to be published).

76. A. Szabo and T. Engel, J. Vac. Sci. Technol. A **12** (1994) 648.

77. G. C. Weaver and S. R. Leone, "Scattering of $Cl_2$ Beams from Si(100) for Kinetic Energies up to 2.6 eV: Implications for Sticking Coefficients and Reaction Product Formation," Surface Sci. (submitted).

78. D. J. D. Sullivan, H. C. Flaum, and A. C. Kummel, J. Phys. Chem. **97** (1993) 12051.

79. F. H. Geuzebroek, Y. Babasaki, M. Tanaka, T. Nakamura, and A. Namiki, Surf. Sci. **297** (1993) 141.

80. A. Szabo, P. D. Farrall, and T. Engel, Surface Sci. **312** (1994) 284.